Springer

KSME

Journal of Mechanical Science and Technology 24 (4) (2010) 923~929
www.springerlink.com/content/1738-494x
DOI 10.1007/s12206-010-0204-z

An experimental study on the performance optimization of a radiant burner with a surface flame structure †

Seung Wan Cho[1], Young Soo Kim[2], Chung Hwan Jeon[3,*] and Young June Chang[3]

[1]*Graduate School of Mechanical Engineering, Pusan National University, Pusan, 609-735, Korea*
[2]*Research Laboratory, LG Electronics, Gaeum jeong-dong, Changwon-city, Gyeongnam, 641-711, Korea*
[3]*Department of Mechanical Engineering, Pusan National University, Pusan, 609-735, Korea*

(Manuscript Received September 28, 2009; Revised December 16, 2009; Accepted December 18, 2009)

Abstract

An experimental study was carried out on a newly developed, gas-fired radiant burner to optimize its performance for three different conditions of firing rate (80.5, 107.4, and 134.2 kW/m^2). The operational equivalence ratios ranged from 0.6 to 1.3. Gas temperatures along the mat and upstream/downstream of the ceramic mat were obtained to investigate the effects of firing rate and equivalence ratio. The temperature of the unburned mixture in the burner port decreased as the firing rate increased. The opposite trend appeared in response to change in the equivalence ratio. This was mainly due to mixture velocity and residence time. The mechanism of temperature variations in the mat with the equivalence ratio and firing rate was described in detail. Results on flue gas emissions, such as the concentrations of EINO and CO, were also presented. It was confirmed that in lean-mixture conditions, the concentration of CO remains below 100 ppm for all firing rates. Lastly, radiation and water-boiling efficiencies were measured as functions of the equivalence ratio, firing rate, cookware diameter (D_p), and height of the burner housing (H). It was observed that conduction heat transport dominated the radiation effect less as the firing rate increased. From these observations, the effective heat input in the present radiant burner was determined to optimize its performance.

Keywords: Radiant burner; Firing rate; Equivalence ratio; Gas temperature; NO and CO emissions; Radiation efficiency; Water-boiling efficiency

1. Introduction

Interest in cleaner combustion has increased significantly in the past few decades. In household appliances, the need for efficient, low-NOx burners has spawned extensive studies on the combustion processes of porous media [1-8]. Ceramics and metal fibers have been widely investigated as porous media due to their high emissivity and high temperature-resistance capability. In general, in a conventional gas-fired burner, the flame and cookware contact directly, which leads to lower combustion efficiency. In contrast, in a radiant burner, the porous medium is heated convectively by the combustion of premixed fuel and air. Convective heat transfer between the gaseous and solid phases is enhanced due to the large ratio of porous media of the surface area to volume, which leads to radiant efficiencies as high as 50%.

Many studies have shown that the emissions of CO and NO are relatively low for lean, premixed, CH_4-air combustion [1-3]. Furthermore, the lower emission of pollutants leads to lower peak temperatures through the stabilization of combustion at a radiation mode than other commercial burners [1]. To design high-efficiency, low-NOx, radiant burners under various burner types and operating conditions, many studies have been undertaken to investigate combustion characteristics, such as the range of stability, radiation efficiency, distribution of the concentration of the mixture close to the mat surface, and emissions [4-6].

Kulkarni et al. [7] carried out an investigation on several kinds of radiant surface burners to examine their radiation and emission characteristics. Their study revealed that a stable flame could be achieved in a wide range of firing rates (200~1200 kW/m^2) and that the radiation efficiency decreased as the firing rate increased. The ranges of flammability and flame stability might be substantially extended due to the incoming fuel/air mixture, which was preheated by radiation and convective heat transfers upstream from the combustion zone [3, 8].

The combustion process in a radiant burner of the premixed, closed type is complicated and highly dependent on many factors, such as the heat capacity, equivalence ratio, geometries of the burner and nozzle, and so on. Therefore, it is very

† This paper was recommended for publication in revised form by Associate Editor Ohchae Kwon

*Corresponding author. Tel.: +82 51 510 3051, Fax.: +82 51 582 9818
E-mail address: chjeon@pusan.ac.kr

difficult to understand fully the mechanism of radiant burner combustion. In the present study, we focused on the evaluation of the combustion characteristics and the performance optimization of a radiant burner. We present experimental measurements of the temperature, NO and CO emissions, and radiation and water-boiling efficiencies. These data will be very useful in designing efficient, low-NOx radiant burners.

2. Experimental methods

2.1 Experimental apparatus

Fig. 1 is a schematic diagram of the experimental apparatus, which consists of two parts: a radiant burner system and a data-acquisition system.

Some details on the burner construction are provided in Fig. 2. The radiant burner assembly was furnished with a ceramic glass cover, burner housing, burner port, ceramic mat, and premixed chamber. The burner housing shaped the outside of the burner assembly and formed a combustion space. The ceramic glass cover was placed on top of the burner housing. A perforated ceramic mat was placed between the burner housing and burner port to enable surface combustion of the mixture, and it served as a radiant body for emitting a radiant wave. A high-temperature gasket was used to prevent leakage. To enable uniform surface combustion throughout the entire ceramic mat, a distribution manifold with 50 holes (d=3 mm) was installed at the lower part of the burner port. A honeycomb-type flow straightener was also adopted in the premixed chamber to ensure uniform mixture distribution and to prevent flashbacks. Brief specifications of the components in the radiant burner are as follows. The diameter and height of the burner housing (resp., port) were 220 and 40 mm (resp., 200 and 25 mm), respectively. The ceramic mat was made of silicon carbide, and its porosity was 95%. The diameter of the mat was 200 mm (the effective diameter is 170 mm), and the thickness was 4 mm. Fuel gas was supplied from the opposite side to improve mixing with air.

The flow rates of air and fuel gas were regulated by a laminar flow meter (LFM) (COSMO Co., DF 2800) and a mass flow meter (MFM) (MILLIPORE Co., FM-3911V), respectively.

The data acquisition system is composed of two subsystems for measuring the emissions and temperatures. The NO and CO emissions were measured at the center of the exhaust port using a NOx analyzer (M-200AH), gas chromatograph (GC) (HP5890 II), and CO analyzer (COPA 2000, Horiba). A water-cooled suction probe (d=2 mm, l=450 mm) was used to obtain the exhaust gas samples.

A schematic diagram of the locations of temperature measurement is presented in Fig. 3. The temperatures inside the burner housing and close to the burner surface were acquired through a Pt/Pt-Rh 13% R-type thermocouple with a bead diameter of 0.3 mm. Measurements were made at nine and eight locations in the horizontal and vertical directions, respectively. To prevent the entry of secondary air from the sur-

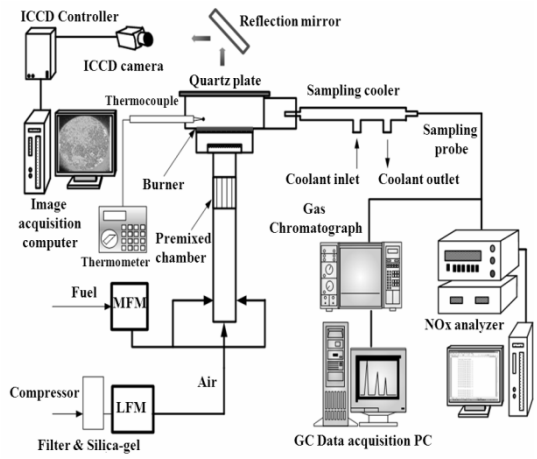

Fig. 1. Schematic diagram of the experimental apparatus.

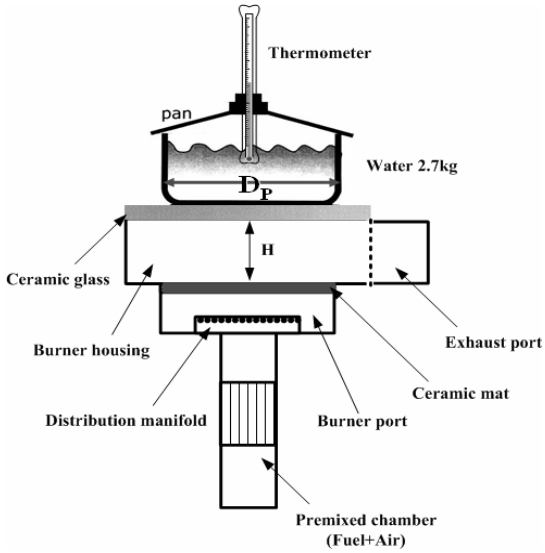

Fig. 2. Schematic diagram of the radiant burner and apparatus for the measurement of water-boiling efficiency.

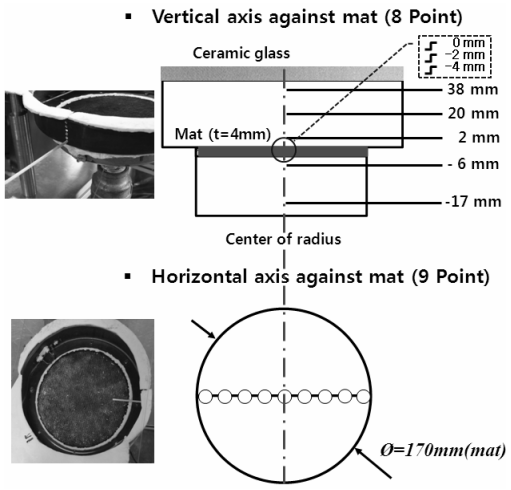

Fig. 3. Schematic of the locations of temperature measurement.

rounding environment, a ceramic glass cover was placed on top of the burner housing.

2.2 Experimental conditions

The radiation efficiency depends primarily on the stabilization characteristics of the premixed flame, which is a strong function of the equivalence ratio and the firing rate.

In this study, the firing rate is defined as follows:

$$Firing\ Rate\ (q) = \frac{\dot{m}_f \cdot HHV}{\rho \cdot A_{eff}} \quad (1)$$

In (1), $\dot{m}_f$ is the mass flow rate of fuel [kg/s], HHV is the higher heating value of fuel [kJ/Nm^3], ρ is the density of natural gas [kg/Nm^3], and A_{eff} is the effective area of the ceramic mat [m^2].

For a fixed firing rate, the equivalence ratio was controlled by changing the air flow rate. For a fixed equivalence ratio, the firing rate was varied by simultaneously changing both the air and fuel flow rates.

The fuel used in this study was natural gas, which was composed of CH_4 (89.95%), C_2H_6 (6.32%), C_3H_8 (2.54%), C_4H_{10} (1.09%), and C_5H_{12} (0.01%). It was supplied with a pressure of 200±50 mmH_2O and a higher heating value of 44,520 [kJ/Nm^3]. The detailed experimental conditions are provided in Table 1.

Table 1. Experimental conditions.

Parameter	Range	
Equivalence ratio, Ø	0.6 ~ 1.3	
Firing rate, q [kW/m^2]	80.5 ~ 134.2	
Temperature measurement	Vertical [mm]	-17 ~ 38
	Horizontal [mm]	-60 ~ +60
Emission analysis	NO_X analyzer	NO_X
	Gas chromatography	CO

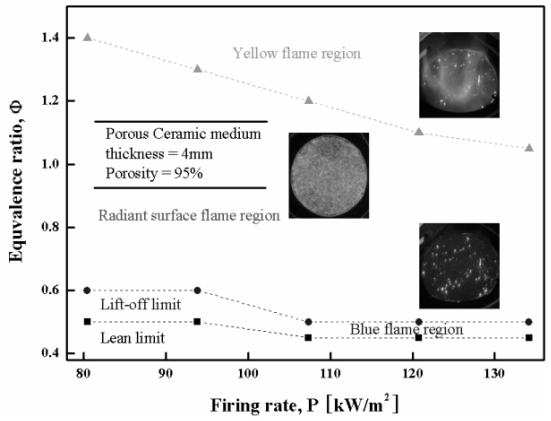

Fig. 4. Flame stability diagram of the present radiant burner.

3. Results and discussion

3.1 Range of flame stability

To determine the operating conditions, the range of flame stability of the radiant burner was investigated. The flame stability diagram of the present radiant burner is shown in Fig. 4. The operating range can be largely divided into three regions: the blue flame region, the radiant surface flame region, and the yellow flame region. At a fixed firing rate, the blue flame arose from the burner's edges as the air flow rate increased. The critical air flow rate was defined as the lift-off limit and was found to manifest at equivalence ratios of 0.5~0.6. Williams et al. [5] also observed that the lift-off from the edges of the burner was due to the higher heat in this region, as a result of which the flame speed was reduced compared with that in the central region. Hwang et al. [9] reported that the blue flame occurred at an equivalence ratio of 0.625 under different conditions of the firing rate (258.5~856 kW/m^2). From these findings, the characteristics of radiant flame stability being highly dependent on the burner design and operating firing rate can be concluded. After reaching the lift-off limit, the air flow rate further increased until the whole flame lifted off the burner surface and was finally extinguished. This was defined as the lean limit of the flame, appearing in the range of 0.45~0.5 with regard to the equivalence ratio. The yellow-flame region could be characterized as the transition of the surface flame to the yellow lift flame in the center of the burner. The yellow-flame region corresponded to a range of 1.05~1.41 for the equivalence ratio and occurred at leaner conditions as the firing rate increased.

3.2 Temperatures

The temperatures acquired at the center points of planes that were parallel to the mat surface are provided in Fig. 5. Measurements were made at five axial locations for three different firing rates, while the equivalence ratio ranged from 0.6-1.1. Details on the locations of measurement are provided in Fig. 3. First, at 6 mm upstream, temperatures of the unburned mixture increasing as the equivalence ratio increased was observed for all firing rates. This was probably due to the lower velocity of the mixture, which consequently resulted in a long residence time for the mixture in the burner port. As the firing rates increased at fixed equivalence ratios, the temperatures decreased due to the short residence time. For the firing rate of 134.2 kW/m^2, the temperatures at the equivalence ratios of 1.0 and 1.1 were almost the same; this could be explained through the above reasons. At the upstream surface of the ceramic mat (at -4 mm), that this trend was retained was also observed.

In the mat, large temperature differences existed between the upstream and downstream surfaces ranging from 560-861°K. The largest temperature difference manifested at a high firing rate (134.2 kW/m^2) and a lean-mixture condition (equivalence ratio of 0.6). This was mainly due to the convective heat transport that resulted from the difference in velocity,

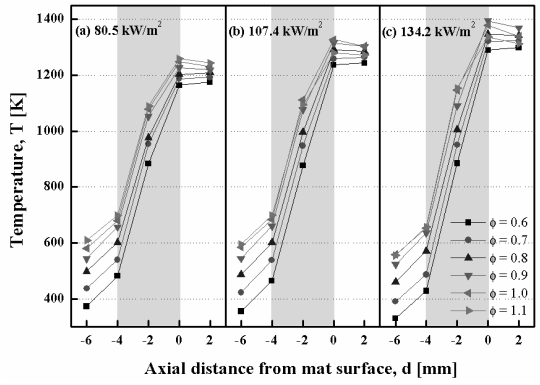

Fig. 5. Temperature profiles obtained at the centers of the parallel planes to the mat surface for three different firing rates.

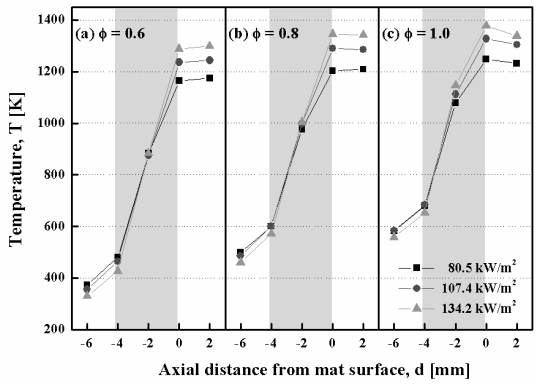

Fig. 6. Temperature profiles obtained at the centers of the parallel planes to the mat surface for three different equivalence ratios.

heat input, and movement of the main reaction zone downstream in accordance with the firing rates [6]. In the former half of the mat (at locations between -4 and -2 mm), at all firing rates and equivalence ratios, the temperature differences were nearly constant at about 400-450°K. However, in the latter half of the mat (at locations between -2 and 0 mm), the temperature differences ranged from 169-405°K. For instance, for the firing rate of 134.2 kW/m^2, the temperature difference was 405°K at the equivalence ratio of 0.6, while it was 184°K at the equivalence ratio of 1.1. At the equivalence ratio of 0.9, 1.0, and 1.1, the temperatures at 2 mm downstream were also lower than those at the surface of the mat (0 mm location). This was mainly due to the movement of the reaction zone to the upstream by the low velocity of the mixture.

The temperatures acquired at the equivalence ratios of 0.6, 0.8, and 1.0 are displayed representatively in Fig. 6. Measurements were made for three different firing rates at the same locations as in Fig. 5. Based on the comparison of the temperature between 0 mm downstream (surface of the mat) and 2 mm downstream, the location of the flame could be predicted. At the stoichiometric condition, for all the three firing rates considered, the temperature at the downstream surface (0 mm downstream) was larger than that at 2 mm downstream. As the mixture became leaner, the temperature at 2 mm downstream exceeded that at the downstream surface of the mat.

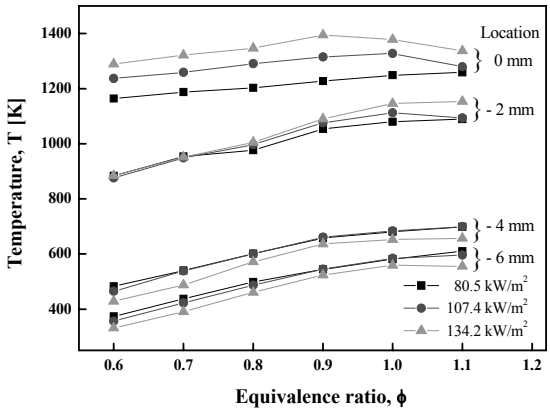

Fig. 7. Gas temperature as a function of the equivalence ratio for three different firing rates at four measurement locations.

This was mainly because the flame moved downstream as the heat input, thus increasing the mixture velocity. The radiation and convective heat transfers from the reaction zone to the mat were reduced as the flame moved downstream, which resulted in a lower temperature of the unburned mixture. In this sense, the minimum temperature of the unburned mixture was found at a firing rate of 134.2 kW/m^2 and equivalence ratio of 0.6. This idea of preheating the mixture can be used successfully to extend the ranges of flammability and flame stability for burning non-flammable mixtures of low heat content, which is also promising from the viewpoints of air pollution and energy recovery [10].

In Fig. 7, for three firing rates and four measurement locations, the gas temperature is shown as a function of the equivalence ratio. The intent was to determine the operating conditions of the radiant burner that optimized the effective heat input. First, at 6 mm upstream, the temperature of the unburned mixture decreased as the firing rate increased. Furthermore, the temperature rise in this upstream region was almost constant at 105°K regardless of the firing rate. At the downstream surface of the mat (0 mm location), the temperature at the firing rates of 80.5, 107, and 134.2 kW/m^2 attained the maximum at the equivalence ratios of 0.9, 1.0, and 1.1, respectively. This was due to the movement of the flame surface according to the velocity of the mixture. From the viewpoint of effective heat input, these conditions were regarded as the optimal operating conditions at the respective firing rates.

Fig. 8 represents the radial temperature distributions at 2 and 38 mm downstream for a fixed firing rate of 134.2 kW/m^2. At 2 mm downstream, a nearly uniform radial temperature distribution was found. The maximum and mean temperatures were 1403 and 1392°K, respectively, at the equivalence ratio of 0.9. At 38 mm downstream, the maximum occurred at an equivalence ratio of 1.0; the corresponding maximum and mean were 1291 and 1273°K, respectively, which were slightly higher than those at the equivalence ratio of 0.9. Generally, the optimal radiant flame depends on the net balance between the energy gained in the preheat region and the energy lost in the reaction zone [2]. Thus, a comparison of the

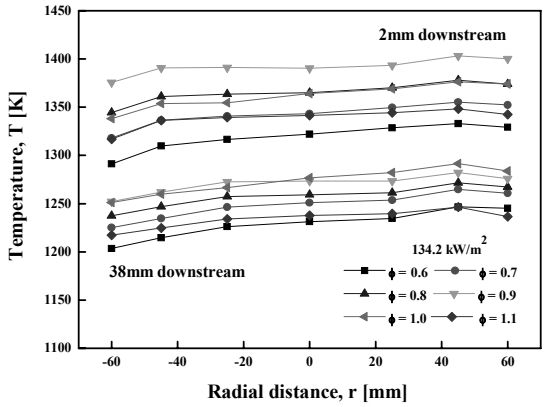

Fig. 8. Radial temperature distributions at 2 and 38 mm downstream under the firing rate of 134.2 kW/m^2.

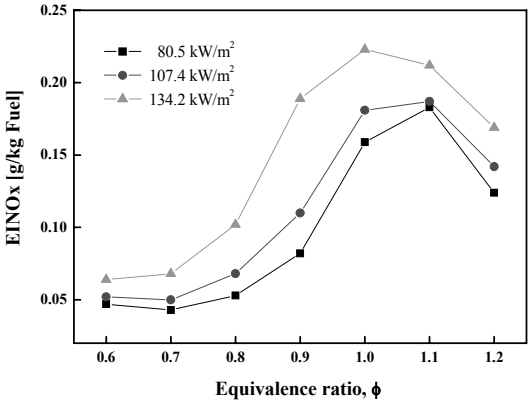

Fig. 9. NO emissions as a function of the equivalence ratio for various firing rates.

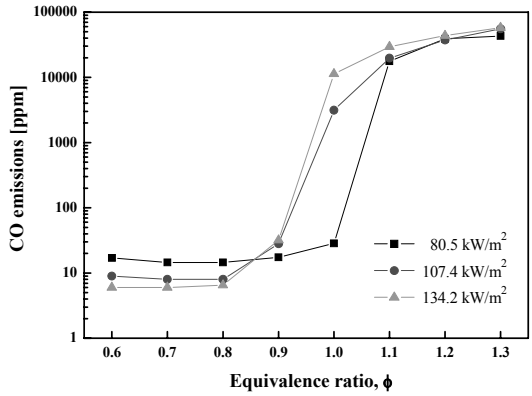

Fig. 10. CO emissions as a function of the equivalence ratio for various firing rates.

two equivalence ratios of 0.9 and 1.0 revealed the latter to be more efficient and closer to optimal. The less-uniform temperature distributions compared with those at 2 mm downstream were due to the burner geometry or the effect of flow to the exhaust port.

3.3 NO and CO emissions

In Figs. 9 and 10, the NO and CO emissions at different firing rates are provided as functions of the equivalence ratio, respectively. The emission rate of species can be normalized by the fuel flow rate, which is commonly defined as follows [11, 12]:

$$EI_i = \frac{m_{i,emitted}}{m_{F,burned}}. \quad (2)$$

$$EINO_X(g/kg) = \frac{X_{NO} + X_{NO_2}}{X_{fuel,i}} \cdot \frac{M_{NO_2}}{M_{fuel}} \cdot 1000. \quad (3)$$

In the above, X_{NO}, X_{NO2}, and $X_{fuel,i}$ are the mole fractions of NO, NO_2, and initial fuel, respectively. M_{NO2} and M_{fuel} are the molecular weights of NO_2 and fuel, and are 46 and 18.12 g/mol, respectively. The NO emissions increased with the firing rate and equivalence ratio because the effective temperature of the reaction zone increased. In the present study, EINO showed slightly higher values (0.05~0.22 g/kg) than those reported in previous studies at equivalent levels of the heat input, which implied that more efficient combustion was achieved [4].

In view of the fact that a large portion of recalls is due to high levels of CO emission during combustion, the reduction of CO emission is an important parameter for designing a new burner. In the present study, the CO emissions were extremely low compared with those at the equivalent level of heat input. In lean-mixture conditions, less CO was emitted than the regulatory value of 1,200 ppm. As the firing rate increased, CO emissions also increased. This was mainly due to a short residence time: an increased firing rate allowed a shorter time for CO to oxidize [2].

3.4 Efficiency

Radiation efficiency (η_R) is one of the most important criteria for evaluating a radiant burner's performance. It is defined as the fraction of input energy converted to radiant energy as follows [12]:

$$\eta_R = \frac{Radiant\ Flux}{Firing\ Rate} = \frac{\varepsilon \cdot \sigma \left(T_G^4 - T_0^4\right)}{q}. \quad (4)$$

In (4), ε is the emissivity (0.95), σ is the Stephan-Boltzmann constant, and T_G and T_0 are the absolute temperatures of the ceramic glass surface and sur-roundings, respectively. An IR Camera (IRCON Inc., 100PHT) was used to measure the surface temperature of the ceramic glass.

In Fig. 11, the radiation efficiency is shown as a function of the equivalence ratio for the three different firing rates. The decrease in the radiation efficiency with the increase in firing rate was probably due to the increased heat loss to the exhaust

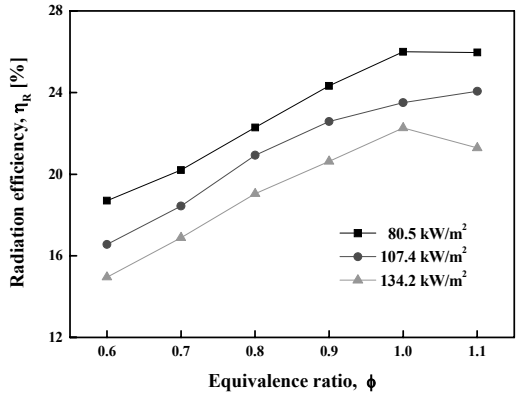

Fig. 11. Radiation efficiency as a function of the equivalence ratio.

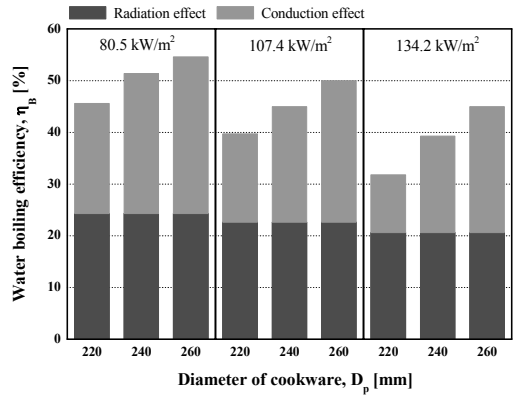

Fig. 12. The water-boiling efficiency as a function of the cookware diameter (D_p) for the three different firing rates (Ø = 0.9).

port, which resulted from the higher velocity of the mixture. It peaked at the stoichiometric condition and gradually decreased with the decrease in equivalence ratio. This was because the burning velocity was maximized at the stoichiometric condition, and the reaction zone was closer to the mat. It was thought that the energy loss to the exhaust port increased as the equivalence ratio decreased. From the observations of the gas temperatures, emission characteristics, and radiation efficiency, the optimal equivalence ratio was considered to exist at a slightly lean condition.

In Fig. 12, the water-boiling efficiency (η_B) at an equivalence ratio of 0.9 is representatively provided as a function of the cookware diameter (D_p) for the three different firing rates. The water-boiling efficiency was defined as the ratio of effective heat transfer, which was obtained using Eq. (5), to the input heat.

$$Q_{eff} = \frac{mC_p\Delta T}{t} = \frac{mC_p(60 - T_i)}{t} \quad (5)$$

In (5), m is the mass of water [kg], C_p is the specific heat [kcal/kgº C], T_i is the initial temperature of water [ºC], and t is the time [s] for heating the water from 20-60ºC. For a comparative study, the mass of water was kept constant at 2.7 kg in the present work. More details on the experimental methods of the water-boiling efficiency can be found at the Korean Standards [13].

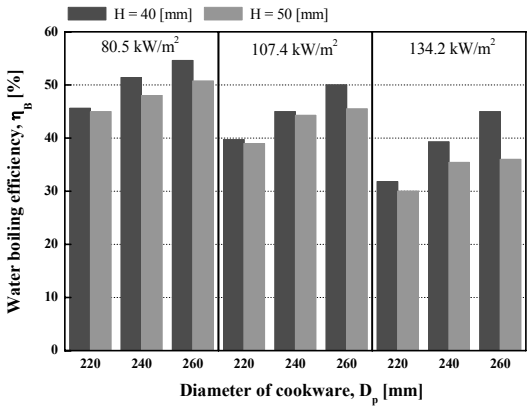

Fig. 13. Effect of the burner housing's height (H) on the water-boiling efficiency for the three different cookware diameters (D_p) and firing rates (Ø = 0.9).

Similar to the radiation efficiency, the water-boiling efficiency decreased with the increase in the firing rate, which was due to the increased heat loss through convection. On the other hand, for any given firing rate, the water-boiling efficiency increased as the cookware diameter (D_p) increased. This was mainly due to the larger conduction heat transfer through the cookware. For instance, when the cookware diameter (D_p) was 220 mm, the water-boiling efficiencies at the firing rates of 80.5, 107.4, and 134.2 kW/m^2 were at 46, 40, and 32%, respectively, while the corresponding radiation efficiencies were at 24.3, 22.6, and 20.6%. Some portion of heat from the ceramic glass would be used to heat the cookware, and convective heat losses might occur from the other sides of the cookware. In this study, however, we assumed that these losses could be negligible. Based on these comparisons, the conduction heat transfer became less dominant than the radiation effect as the firing rate increased, which was mainly due to the larger losses of energy to the exhaust port. One aim of this study was to determine the effective heat input in the present radiant burner for optimizing the performance. Based on these viewpoints, the firing rate of 107.4 kW/m^2 was regarded as an optimal condition in the present burner-geometry for meeting our target water-boiling efficiency of 40%.

In Fig. 13, the effect of the height of the burner housing (H) on the water-boiling efficiency is displayed by varying the height from 40 to 50 mm. The firing rate increased, while the water boiling efficiency decreased. Furthermore, the water-boiling efficiency at a cookware height (H) of 220 mm decreased by less than 2% as H varied from 40 to 50 mm, while it decreased up to 9% at a cookware height of 260 mm. From these results, the combined effect of the cookware diameter (D_p) and the height of the burner housing (H) on the water-boiling efficiency could be observed.

4. Conclusions

The following conclusions can be drawn from the present study of a gas-fired radiant burner for three different firing rates as a function of the equivalence ratio:

(1) The temperature of the unburned mixture in the burner port (upstream) decreased as the firing rate increased, while the opposite trend was observed as the equivalence ratio increased. The largest temperature differences between the upstream and downstream surfaces could be found at lean mixtures and high firing rates; the difference reached up to 861 K.

(2) The NO emissions increased with the firing rate and equivalence ratio. The CO emission also increased with the firing rate. In the present study, CO emissions were extremely low compared with those at the equivalent level of heat input. In lean-mixture conditions, the concentration of CO dropped below 100 ppm for all firing rates, which was satisfactory in relation to the regulatory value.

(3) The radiation efficiency decreased with the increase in firing rate and decrease in equivalence ratio. The heat transport mechanism could be identified as a function of the firing rate. Finally, the effective heat input for optimizing performance in the present radiant burner could be determined.

Acknowledgment

This work was supported by LG Electronics. The radiant burner was authorized as an Excellent Korean Technology by the Ministry of Education, Science and Technology (MEST) of the Republic of Korea in 2005.

References

[1] R. Mital, An experimental and a theoretical investigation of combustion and heat transfer characteristics of reticulated ceramic burners, *Ph.D thesis*, Purdue University (1996).

[2] M. R. Kulkarni, Radiant surface burner performance a numerical and experimental study, *Ph.D thesis*, Arizona state University (1996).

[3] R. Echigo, Y. Yochizawa, K. Hanamura and T. Tomimura, Analytical and experimental studies on radiative propagation in porous media with internal heat generation, *Proc. of 8th International Heat Transfer Conference*, 2 (1986) 827-832.

[4] R. Mital, J. P. Gore and R. Viskanta, A Study of the structure of submerged reaction zone in porous ceramic radiant burners, *Combustion and Flame*, 111 (1997) 175-184.

[5] A. Williams, R. Woolley and M. Lawes, The formation of NOx in surface burners, *Combustion and Flame*, 89 (1992) 157-166.

[6] O. Kawaguchi, A. Todoroki and Y. Murayama, Premixed combustion at a fiber mat, *Twenty-Third Symposium on Combustion, The Combustion Institute*, (1990) 1019-1024.

[7] M. R. Kulkarni, K. P. Chavali and R. E. Peck, Emission characteristics of radiant surface burners, *Proc. of the western states section of the combustion institute, October* 12-13 (1992).

[8] D. K. Min and H. D. Shin, Laminar premixed flame stabilized inside a honeycomb ceramic, *Int. J. Heat Mass Transfer*, 34 (2) (1991) 341-356.

[9] S. S. Hwang, Combustion and emission characteristics of the surface flames in porous ceramic burner, *Journal of the Korean Society of Combustion,* 6 (1) (2001) 29-35.

[10] F. J. Weinberg, Combustion Temperatures, Nature, (233) (1971) 239-241.

[11] S. R. Turns, An introduction to combustion: concepts and applications, *2th McGraw-Hill series in mechanical engineering*, McGrqw-Hill (1999).

[12] M. D. Rumminger, Numerical and experimental investigation of heat transfer and pollutant formation in porous direct fired radiation burners, *Ph.D thesis*, University of California-Berkeley (1996).

[13] KS (Korean Industrial Standards) B 8115, Gas burning oven range, KS B 8101 (Performance of oven range: Thermal efficiency) (2008) 14-16.

Seung Wan Cho received his M.S. and Ph.D degrees from the department of Mechanical Engineering, Pusan National University, KOREA, in 2003 and 2009, respectively. Dr. Cho is currently a visiting Professor at the School of Automobile at Busan College of Information Technology in Busan, Korea. His research interests include internal combustion engines, stratified combustion and Bi & Dual fuel Engine.

Chung-Hwan Jeon is Professor of Mechanical Engineering at the Pusan National University since March 1998. Prior to coming to PNU, he was a researcher at the Korea Institute of Machinery and Materials (KIMM) through 1992, post doctoral researcher at the Pennsylvania State University through 1995 and principal investigator at the Sam-Sung Aerospace Industries through 1996. Jeon has worked primarily in the fields of combustion and energy conversion system since receiving Ph.D. from Pusan National University in 1994. Advanced laser diagnostics, such as CARS, LIF, LII, are used to investigate these phenomena.